

## Experimental proof of the electronic charge-transfer mechanism in a $\text{YBa}_2\text{Cu}_3\text{O}_{7-x}$ -based field-effect transistor

V. Talyansky, S. B. Ogale, I. Takeuchi, C. Doughty, and T. Venkatesan

Center for Superconductivity Research, Department of Physics, University of Maryland, College Park, Maryland 20742

(Received 30 November 1995; revised manuscript received 31 January 1996)

The dynamics of charge transfer in a  $\text{YBa}_2\text{Cu}_3\text{O}_{7-x}$ -based field-effect transistor were studied in the normal state using signal shape analysis and frequency mixing techniques, the latter being the most sensitive means of measuring field effect utilized so far. The speed of response was found to be limited only by the  $RC$  time constant of the device configuration ( $\sim 9 \mu\text{sec}$ ). Also the electric field modulation of the channel resistance was unchanged from dc to the highest frequency achieved in this device, showing the absence of any significant "slow" component. This observation unambiguously demonstrates that direct field induced modulation of the charge carrier density plays a major role in the relatively fast electric field effect in metal-oxide superconductors. [S0163-1829(96)04921-1]

Studies of electric field effects in high- $T_c$  superconductors and the related development of SuFET (superconducting field-effect transistor) structures have recently attracted considerable attention because of scientific and technological implications. Fiory *et al.*<sup>1</sup> studied the field induced modulation of resistance and superconducting kinetic inductance via capacitive charging of (001) surfaces in  $\text{Y}_1\text{Ba}_2\text{Cu}_3\text{O}_{7-x}$  (YBCO) and obtained such parameters as the mobility, density, and effective mass of carriers in the system. Mannhart *et al.*<sup>2</sup> demonstrated that the pinning force and critical current density in YBCO films can be controlled by the electric field and attributed this observation to changes in the density of mobile carriers. Xi *et al.*<sup>3</sup> examined the field effect in (1–8)-unit-cell-thick films of YBCO and revealed differences in the effect of hole filling on the normal state and superconducting transport. Walkenhorst *et al.*<sup>4</sup> studied the vortex dynamics of ultrathin YBCO films and demonstrated tunability of a Kosterlitz-Thouless type transition (observed in zero magnetic field) by the electric field. Mannhart *et al.*<sup>5</sup> in their subsequent studies reported large electric field effects in YBCO films containing weak links, with a reduction of  $T_c$  by 10 K or more, for an applied field of 6 MV/cm.

Insofar as the technological aspects are concerned, it has already been shown that an applied electric field can be used to demonstrate FET characteristics<sup>1–3</sup> as well as to tune the properties of thin-film superconducting inductors used in superconducting quantum interference device based applications<sup>6</sup> and microwave devices.<sup>7</sup> The availability of superconducting three-terminal devices may be valuable for certain digital electronics application, provided that such devices can quickly switch on and off the superconducting transport with signal gain and low power loss.

Even though most of the studies mentioned above imply that the cause of the electric field effect in high- $T_c$  superconductors is modulation of the density of mobile carriers, the manner in which this change comes about has caused a great deal of debate.<sup>1–3,8–11</sup> The origin of field effect has been attributed to both charge carrier transfer<sup>2,3,11,12</sup> and the reorganization of Cu-O bonds by the movement of oxygen ions, causing the carrier concentration in the planes to change.<sup>8</sup> These viewpoints differ in their predictions primarily in the

context of the response times of the observed effects: the response associated with oxygen dynamics is expected to be considerably slower than that defined by the electronic mechanism of charge transfer. Resolving this issue is extremely important to fully understand the fundamental physics behind the electronic transport in YBCO having in mind that it has make-or-break implications for the success of SuFET utilization in superconducting electronics.

Our experiments were performed on a SuFET trilayer structure formed by a YBCO channel layer, an insulating  $\text{SrTiO}_3$  (STO) layer, and a gold metallization layer that provided contact to the source, drain, and gate of the device, as shown in Fig. 1(a). The entire structure was deposited *in situ* and then patterned by laser ablation using a metal mask into a four-probe configuration shown in Fig. 1(b); then the gate metallization was separated from that of source and drain by wet-etching. Details of the device fabrication have been published elsewhere.<sup>13</sup>

The gate capacitance was about 1.7 nF at 40 K measured with an HP4261A LCR meter, and the gate area was around 0.3 mm<sup>2</sup> yielding the dielectric constant  $\epsilon \approx 310$ . The dielectric parameters of such modest quality thin STO films are known to be weakly field and temperature dependent,<sup>7,14</sup> and we neglected any such dependence in this work. The gate leakage current was 1 nA under gate voltages +11 and –6 V at 20 K. The channel superconducting transition ( $R_{\text{ch}}=0$ ) was observed at 30 K. A square wave signal with amplitude of about 8 V was applied to the gate by an HP8111A pulse/function generator, the channel current bias of 1 mA was applied with a Keithley 224 programmable current source, and the channel response was monitored with a Tektronix 7623A oscilloscope connected as shown in Fig. 2. The device was cooled in a helium-flow cryostat, where the temperature was controlled with a Lake Shore DRC 93CA controller.

The applied gate voltage and zero current biased channel response signals are shown in Fig. 3(a). As expected, the channel response signal appears to be a result of differentiation of the gate input signal. The vertical slopes of the gate input square wave are transformed into positive and negative spikes present in the channel response. The spikes exponen-

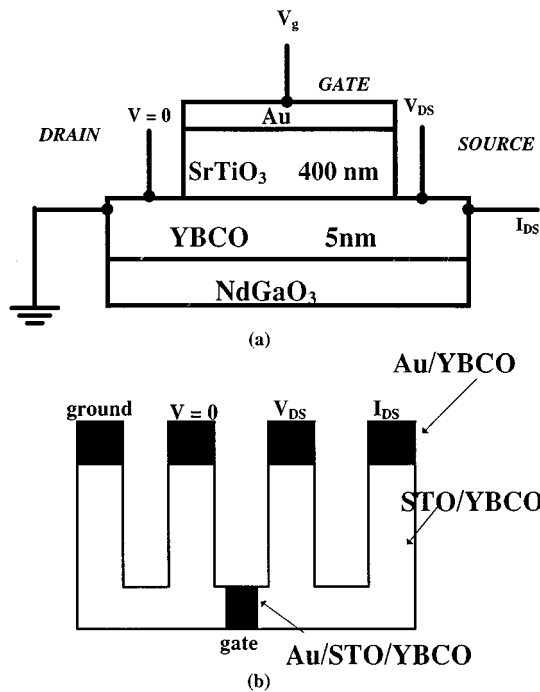


FIG. 1. (a) The schematic cross section of a typical SuFET patterned from a deposited *in situ* Au/STO/YBCO multilayer into a four-probe configuration; (b) the schematic planar view of the device.

tially decay down to the flat regions of the response. Any two adjacent flat regions of the response signal correspond to positive and negative values of the gate voltage. As we know, field effect is manifested in changing values of the channel resistance dependent on the applied gate voltage bias. The change in the channel resistance could be detected by measuring the voltage across a current biased channel. The channel current bias changing from zero to  $i_b = 1$  mA causes the two adjacent flat regions of the response signal to separate vertically on the oscilloscope's screen by the amount of  $2\Delta v = i_b \Delta R$  as shown in Fig. 3(b). Also the channel current bias shifts the entire signal plot up by  $v_0 = i_b R_0$ , where  $i_b$  is the bias current,  $\Delta R$  is the difference in the channel resistances, and  $R_0$  is the channel resistance at zero gate bias. By reading  $v_0$  and  $\Delta v$  off the oscilloscope we could find the resistance modulation  $\gamma = \Delta v / v_0 = \Delta R / R_0$ . The leakage current contribution to the response signal exceeded the

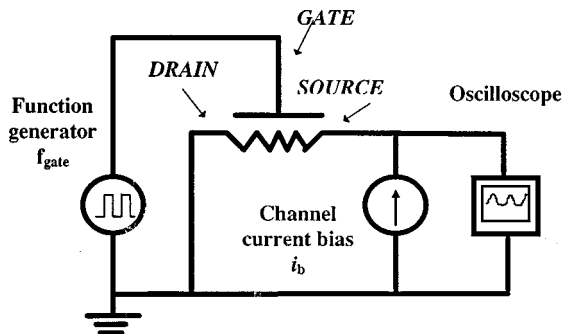


FIG. 2. The measurement setup for studying the YBCO channel response in the normal state under an ac gate bias.

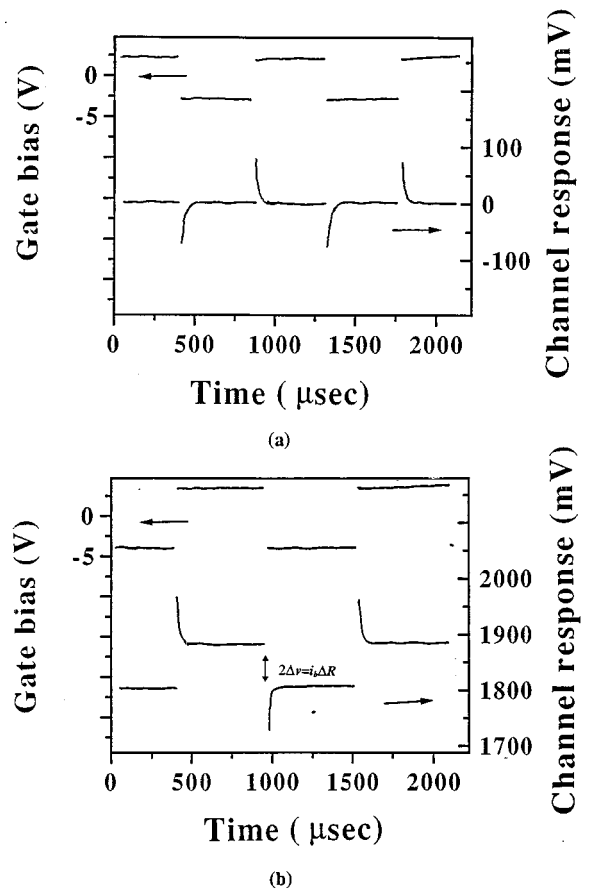


FIG. 3. (a) The gate input signal and the zero-biased channel response; (b) the gate input signal and the 1 mA dc current-biased channel response.

measurement error at relatively high temperatures and could be accounted for by measuring the separation between the two consecutive flat regions of the response signal at zero channel current bias. The resistance modulation  $\gamma$  was measured by the method discussed above for a temperature range from 30 K up to 90 K. The device exhibited a usual temperature dependence of the modulation that rose sharply as the temperature was lowered down to  $T_c$  as shown in Fig. 4. At a given stabilized temperature the frequency of the input sig-

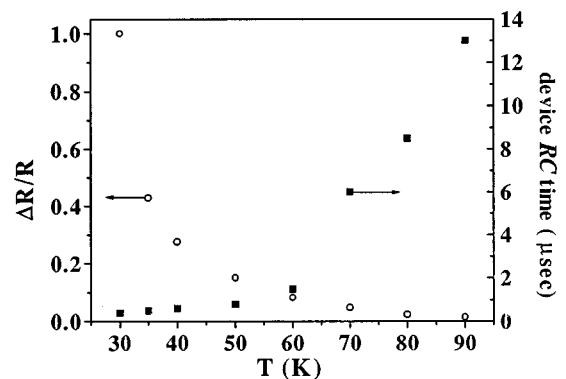


FIG. 4. The temperature dependences of the channel resistance modulation  $\Delta R/R$  and of the device RC time. The shape analysis method limits the speed of the field-effect detection to the device operating frequency lower than  $(10RC)^{-1}$ .

nal was varied from dc up to a detection limit frequency dependent on the temperature.

The method described above of evaluating  $\gamma$  is based on our ability to recognize the flat regions of the response signal, which are shrinking due to the fixed  $RC$  time as the input gate frequency increases. The spikes in the channel response resulting from differentiating the vertical slopes of the input exponentially decay down to 99% of their maximal value within a time period of  $5RC$ . Thus the detection limit frequency is about  $(10RC)^{-1}$  that varies with temperature due to the changing channel resistance. The temperature dependence of the time constant  $RC$  is shown in Fig. 4. We found that the channel resistance modulation stayed constant within the experimental error for each given temperature of measurement over the frequency range limited at such temperature as discussed above. Because of the measurement method limitations of the shape analysis technique, we were able to achieve operating speeds of the device only up to 25 kHz at the transition temperature with a current biased channel.

Recently the results of a similar experiment were published by Shneider and Auer,<sup>15</sup> where a fast SuFET operation that was supported with data obtained using the shape analysis technique was reported. An estimate of the field effect time scale of less than  $0.3 \mu\text{sec}$  was deduced from the temporal width of the charging spike in the channel response signal (similar to the ones shown in Fig. 3). The authors derive this time scale from the charging spike while driving the device with a square wave function gate voltage, whose period is  $100 \mu\text{sec}$ . The problem with this shape analysis method is that it is inherently limited to a rough evaluation of the positions of the oscilloscope plot points amid background noise, cable echo, and other irregularities of the measurement circuit. The method does not provide an accurate means of determining the time scale of the field-effect response of the device. To overcome the limitations of the shape analysis method, we developed an approach of frequency mixing in a field-effect device. As will be demonstrated by the result and as is widely known in the theory of measurements, studies in the frequency domain are superior in sensitivity as compared to the signal shape studies we carried out earlier.

The device featured a 5 nm thick, 1 mm long, and 0.5 mm wide YBCO channel with a superconducting transition at  $T_c = 49 \text{ K}$  ( $R_{\text{ch}} = 0$ ). The gate capacitor  $C_g \approx 3 \text{ nF}$  (measured with an electrometer) consisted of a 400 nm thick STO layer and had an area of  $0.5 \text{ mm}^2$  giving a dielectric constant  $\epsilon_r \approx 270$ . The measurement circuit is shown in Fig. 5. The resistance of  $R_c = 3 \text{ k}\Omega$  (at  $T = 50 \text{ K}$ ) originates from the leads connecting the contact pad with the device channel [see Fig. 1(b)]. The capacitor  $C_p \approx 400 \text{ pF}$  represents the parasitic capacitance of the cable and wiring.

Our measurement method exploits the fact that two signals of different frequencies  $f_g$  and  $f_b$  passing through a nonlinear circuit element will mix, with the result that signals of frequencies equal to the difference  $f_g - f_b$  and the sum  $f_g + f_b$  of the primary frequencies as well as numerous other differences and sums of the secondary low-magnitude signals (harmonics) are produced. In our case such a nonlinear element is the YBCO channel in the normal state whose resistance is modulated by the voltage applied to the gate  $v_g \sin(2\pi f_g t) + v_{g0}$  and measured by the channel bias cur-

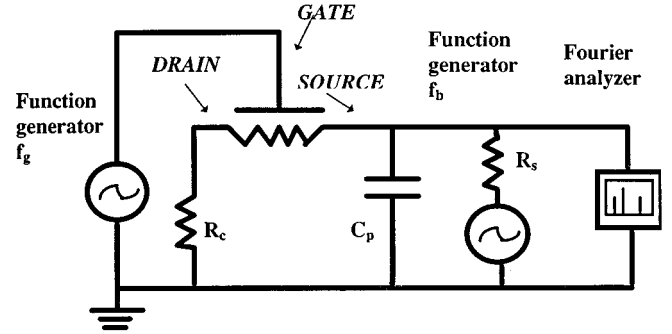


FIG. 5. The frequency mixing measurement setup utilizing one function generator to modulate the channel through the gate at frequency  $f_g$ , another function generator to current bias the channel at frequency  $f_b$ , and a Fourier analyzer as the detector of SuFET's response.

rent  $i_b \sin(2\pi f_b t)$ . As it was found earlier by Xi *et al.*,<sup>3</sup> who relied on the charge-transfer model of field effect, the relative change in the channel resistance is proportional to the relative change in the number of the channel charge carriers:

$$\begin{aligned} -\Delta N/N &= \Delta R_{\text{ch}}(t)/R_{\text{ch}}^0 = (C_g/edAn)v_g \sin(2\pi f_g t) \\ &= \gamma v_g \sin(2\pi f_g t), \end{aligned}$$

where  $A$  is the gate area,  $d$  the channel thickness,  $R_{\text{ch}}^0$  the channel resistance at the gate voltage offset  $v_{g0}$ , and  $n$  the channel charge carriers volume density at the gate voltage offset  $v_{g0}$ ;  $\gamma$  reflects the degree of modulation. Neglecting the presence of  $R_c$  and  $C_p$  to simplify derivation, we can write the source-drain current  $i_{\text{ds}}(t)$  as a sum of the channel bias current and the gate charging current:

$$i_{\text{ds}}(t) = i_b \sin(2\pi f_b t) + 2\pi v_g C_g f_g \cos(2\pi f_g t).$$

Then having a time-dependent channel resistance

$$R_{\text{ch}}(t) = R_{\text{ch}}^0 + \Delta R_{\text{ch}}(t) = R_{\text{ch}}^0 \{1 + \gamma v_g \sin(2\pi f_g t) + v_{g0}\},$$

we expect the source-drain voltage to be

$$\begin{aligned} v_{\text{ds}}(t) &= i_{\text{ds}} R_{\text{ch}} \\ &= \{i_b \sin(2\pi f_b t) + 2\pi v_g C_g f_g \cos(2\pi f_g t)\} R_{\text{ch}}^0 \\ &\quad \times \{1 + \gamma v_g \sin(2\pi f_g t) + v_{g0}\}. \end{aligned}$$

The sum and difference frequencies ( $f_g \pm f_b$ ) can be present in the drain-source voltage only if the gate voltage modulates the channel resistance ( $\gamma$  is different from zero), with the voltage amplitude at the difference/sum frequencies  $\gamma v_g i_b R_{\text{ch}}^0 / 2 = i_b \Delta R_{\text{ch}} / 2$  being proportional to the amount of modulation per gate bias volt,  $\gamma$ . As it could be seen from the above equations, a dc offset  $v_{g0}$  applied to the gate would not effect the response signal amplitude at the difference/sum frequencies.

The frequency mixing measurement required two function generators and a Fourier analyzer as the signal detector. A sinusoidal gate voltage of frequency  $f_g$  was swept between the values of 0 and 12 V with one of the generators. These values were chosen to keep the gate leakage current below 1 nA. Also operating in the positive gate voltage range allows

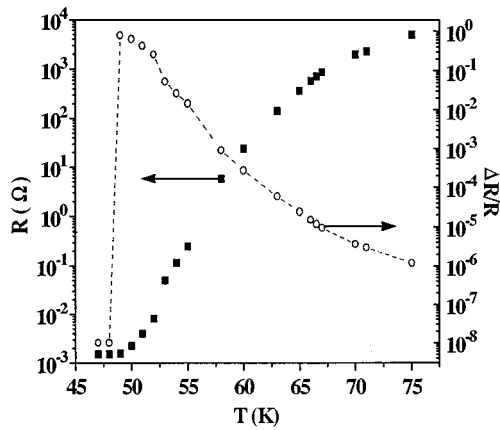


FIG. 6. The temperature dependencies of the channel resistance  $R_{\text{ch}}^0$  (solid squares) and the resistance modulation  $\Delta R_{\text{ch}}/R_{\text{ch}}^0$  (open circles).

us to move away from the STO nonlinear region lying just below 0 V.<sup>14</sup> The other generator was used to apply a current bias of frequency  $f_b$  and amplitude  $160 \mu\text{A}$  to the channel of the device, with  $R_s = 100 \text{ k}\Omega$  connected in series to make the generator a reliable current source. The Fourier analyzer displayed the frequency spectrum of the drain-source voltage on a scale up to a maximum of 100 kHz after averaging the spectrum 20 times. The device was mounted on the cold finger of a continuous helium flow cryostat with temperature control.

As the temperature was decreased below  $T_c = 49 \text{ K}$  ( $R_{\text{ch}} = 0$ ), the peak in the spectrum situated at the difference frequency  $(f_g - f_b)$  dropped in magnitude sharply down to the noise level. This is indicative of the absence of field induced resistance modulation in the superconducting channel as expected. We have found that the magnitude of the difference peak is a dependable measure of the channel modulation, since the modulation is the major mechanism of getting an output involving mixed input frequencies as we derived earlier, assuming that other nonlinear effects in the circuit are too small for detection. Although the channel characteristics exhibit a slight nonlinearity just above the transition temperature, we have observed that the two current signals of different frequencies introduced into the channel without involving the gate do not produce the mixing peaks distinguishable from the noise level. Hence we conclude that if there are any mixing peaks due to the nonlinearity of the channel, they must be at least two orders of magnitude smaller than the same peaks produced by the mixing through the gate. Furthermore, the evidence of the minimal effect of the nonlinearity of the channel is given by the absence of the signal at  $(f_g - f_b)$  in the measurement of the channel in the superconducting state, where the nonlinearity is expected to be even stronger than that above the transition as shown in Fig. 6. Another possible source of nonlinearity is charge trapping. The charge trapping of a considerable magnitude has not been observed in the SuFET device reported. If it had been present in our devices, we would have observed hysteresis in the plot of the channel resistance as a function of the gate bias voltage. This was not the case in our experiments within the instrument error.

We related the height of the difference peak at

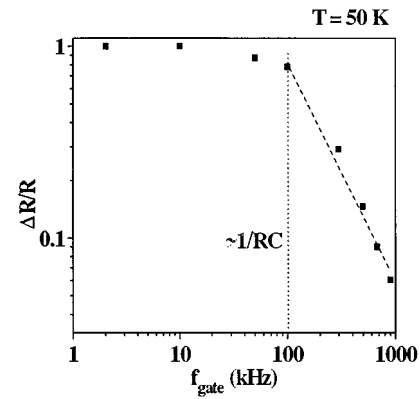


FIG. 7. The frequency response of a SuFET with  $RC \approx 9 \mu\text{sec}$  driven at gate frequency up to 1 MHz. The dotted line marks the position of frequency  $1/RC \approx 100 \text{ kHz}$ , and the dashed line indicates the roll-off slope of 20 dB/decade.

$(f_g - f_b) = 21 \text{ kHz}$  in the output frequency spectrum to the change in the channel resistance  $\Delta R_{\text{ch}}$  as was derived above, having the gate input frequency  $f_g = 91 \text{ kHz}$  and channel current bias frequency  $f_b = 70 \text{ kHz}$ . The dependence of the channel resistance  $R_{\text{ch}}^0$  and its modulation  $\Delta R_{\text{ch}}/R_{\text{ch}}^0$  on temperature in the region close to  $T_c$  are shown in Fig. 6. Because  $R_c$  was temperature dependent, the modulation was calculated using  $R_{\text{ch}}^0$  values of a separately measured  $R$  vs  $T$  curve instead of the peak value at  $f_b$  as is suggested by the derivation. As has been previously found,<sup>4</sup>  $\Delta R_{\text{ch}}/R_{\text{ch}}^0$  rises as the temperature is reduced to  $T_c$ . For  $f_g$  much lower than 91 kHz the degree of modulation stayed practically constant being equal to about unity at  $T = 50 \text{ K}$  from a dc measurement ( $f_g = 0$ ,  $v_g = 12 \text{ V}$ ). It could be seen from Fig. 6 that frequency mixing is a very sensitive technique capable of detecting resistivity modulations at least as small as  $10^{-6}$ . We investigated the frequency response of the device at  $T = 50 \text{ K}$  at higher driving frequencies  $f_g$  up to 1 MHz by keeping the difference frequency  $f_g - f_b$  in the allowable observation range below 100 kHz. The amount of modulation did not change appreciably up to a point at  $f_g \approx 100 \text{ kHz}$  and then started to roll off as shown in Fig. 7. The position of this turning point can be explained by calculating the  $RC$  constant of the device configuration which is  $R_c C_g = 3 \text{ k}\Omega \times 3 \text{ nF} = 9 \mu\text{sec}$  which is close to  $(100 \text{ kHz})^{-1}$ . Also the slope of the decrease in modulation is around 20 dB/decade as indicated in Fig. 7, the kind of behavior we would expect from an electronic device driven at speeds exceeding its  $1/RC$  limit.

The results shown in Fig. 7 suggest that the amount of the field induced modulation in a SuFET is constant for gate frequencies below the  $1/RC$  value of the device at a given temperature. This means that for the studied frequency range, the device operational speed is limited only by the parameters affecting the  $RC$  product rather than any intrinsic time constants associated with transport and charge modulation in YBCO. Employing conventional lithographic patterning techniques one should easily be able to fabricate micron-size SuFET's with  $RC$  constants reduced to less than a nanosecond. We cannot, of course, rule out the possibility that in the corresponding (microwave) frequency range various hitherto unrevealed transport mechanisms may surface

and limit the operational speed of the device. This is an exciting direction for another detailed study that could provide valuable information on high-frequency transport phenomena in YBCO. While the present experimental method only allows for measurements in the resistive state of the YBCO channel, we have no reason to believe that the underlying dynamics that determine the device response time are different in the superconducting state. This work demonstrates the fastest device performance reported in a SuFET so far and raises hopes for achieving even higher speeds.

Now we discuss the significance of our results in the context of the debate regarding the mechanism of electric field effects in high- $T_c$  superconductors. As we mentioned earlier, there are two competing viewpoints on the matter: one attributes the effects to charge transfer while the other to reorganization of oxygen bonding in the Cu-O chains and consequent changes in the density of mobile carriers in the Cu-O plane system. In our view both aspects are present in the effect, the key question being their relative contributions and their response times.

The oxygen ordering model suggested by Chandrasekhar *et al.*<sup>8</sup> appears to successfully explain the data on photoinduced charges in the normal state and superconducting properties of YBCO,<sup>16</sup> as well as charging effects in partially oxygen-depleted superconducting YBCO and the corresponding behavior under aging and hydrogen doping.<sup>16</sup> However, as emphasized by Kula *et al.*<sup>17</sup> and Frey *et al.*,<sup>11</sup> the applicability of the oxygen reordering model to Bi and Tl based systems, which do not have loosely bound oxygen, but which have displayed field effects, is not clear. The oxygen reordering model also demonstrates that the origin of the asymmetry of the response shown in the Monte Carlo simulation<sup>8</sup> evidently lies in the choice of the difference in the density of “up” and “down” dipoles. However, there appears to be no obvious physical reason for their asymmetry in a free standing superconducting crystal. In a thin film deposited on a substrate one could invoke the notion of a strain field and related polarization anisotropies, but the model does not comment on how this will be accomplished in real systems in a quantitative way. In support of the validity of their argument and against the charge-transfer model, Chandrasekhar *et al.*<sup>8</sup> have pointed out that the experimentally observed response in the experiments of Manhart *et al.*<sup>5</sup> and Xi *et al.*<sup>12</sup> was much slower than the calcu-

lated  $RC$  time constants which were of the order of microseconds. The results of our present studies unambiguously demonstrate that superconducting devices do respond on a microsecond time scale set by the  $RC$  time constant. This shows that in the field effect in high- $T_c$  superconductors, charge transfer not only occurs but also constitutes the dominant mechanism, since the effect can be observed on electronic time scale rather than the oxygen ion hopping time scale predicted by the oxygen reordering model to be of the order of minutes. We, however, insist that it would be inappropriate to seek the origin of all field induced phenomena in one or the other mechanism. As some evidence shows, the slower effects can be attributed to oxygen reordering while the faster ones to charge transfer. Nevertheless, the amount of modulation is found to be the same for an ac gate bias of 100 kHz as that for a dc gate bias ( $f_g=0$ ,  $v_g=12$  V) applied for as long as 15 min. Thus we believe that the “slow” component of the field effect associated with oxygen migration plays an insignificant role if any in the phenomena detected by the measurements that are done on a time scale of seconds to minutes. Still the oxygen migration mechanism could be contributory to “ultraslow” phenomena like the one observed by a 40-h long measurement in Ref. 17. It would be interesting to understand whether the slower effects can also be related to charge induced changes in the local electronic states and resulting changes in oxygen ordering.

In conclusion, by using a frequency mixing method applied to a SuFET structure, we have shown that the operational device speeds which can be realized in electric field effects in high- $T_c$  superconductors are limited only by the device  $RC$  time constant, and there is no manifested intrinsic limitation originated in the material system itself within the investigated frequency range (up to 1 MHz). Our observation does not, however, exclude the possible effects of relatively slow phenomena involving structural changes such as oxygen ordering, but recognizes their minor role in faster processes occurring on the time scale shorter than minutes.

The authors appreciate useful discussions with A. T. Findikoglu, S. M. Anlage, and P. A. Warburton. We are also grateful to M. Rajeswari for assistance in measurements. We would like to acknowledge support from NSF Grant No. DMR 9404579.

<sup>1</sup>A. T. Fiory, A. F. Hebard, R. H. Eick, P. M. Mankiewich, R. E. Howard, and M. L. O'Malley, *Phys. Rev. Lett.* **65**, 3441 (1990).  
<sup>2</sup>J. Mannhart, D. G. Schlom, J. G. Bednorz, and K. A. Muller, *Phys. Rev. Lett.* **67**, 2099 (1991).  
<sup>3</sup>X. X. Xi, C. Doughty, A. Walkenhorst, C. Kwon, Qi Li, and T. Venkatesan, *Phys. Rev. Lett.* **68**, 1240 (1992).  
<sup>4</sup>A. Walkenhorst, C. Doughty, X. X. Xi, Qi Li, C. J. Lobb, S. N. Mao, and T. Venkatesan, *Phys. Rev. Lett.* **69**, 2709 (1992).  
<sup>5</sup>J. Mannhart, J. Strobel, J. G. Bednorz, and Ch. Gerber, *Appl. Phys. Lett.* **62**, 630 (1993).  
<sup>6</sup>Y. Gim, C. Doughty, X. X. Xi, A. Amar, T. Venkatesan, and F. C. Wellstood, *Appl. Phys. Lett.* **62**, 3198 (1993).  
<sup>7</sup>A. T. Findikoglu, C. Doughty, S. M. Anlage, Qi Li, X. X. Xi, and

T. Venkatesan, *Appl. Phys. Lett.* **63**, 3215 (1993).  
<sup>8</sup>N. Chandrasekhar, O. T. Valls, and A. M. Goldman, *Phys. Rev. Lett.* **71**, 1079 (1993).  
<sup>9</sup>A. A. Aligia, *Phys. Rev. Lett.* **73**, 1561 (1994).  
<sup>10</sup>N. Chandrasekhar, O. T. Valls, and A. M. Goldman, *Phys. Rev. Lett.* **73**, 1562 (1994).  
<sup>11</sup>T. Frey, J. Mannhart, J. G. Bednorz, and E. J. Williams, *Phys. Rev. B* **51**, 3257 (1995).  
<sup>12</sup>X. X. Xi, C. Doughty, A. Walkenhorst, S. N. Mao, Qi Li, and T. Venkatesan, *Appl. Phys. Lett.* **61**, 2353 (1992).  
<sup>13</sup>C. Doughty, Ph.D. thesis, University of Maryland, 1994.  
<sup>14</sup>K. Petersen, I. Takeuchi, V. Talyansky, C. Doughty, X. X. Xi, and T. Venkatesan, *Appl. Phys. Lett.* **67**, 1477 (1995); A. T.

Findikoglu, C. Doughty, S. M. Anlage, Qi Li, X. X. Xi, and T. Venkatesan, *J. Appl. Phys.* **76**, 2937 (1994); A. Walkenhorst, C. Doughty, X. X. Xi, S. N. Mao, Qi Li, R. Ramesh, and T. Venkatesan, *Appl. Phys. Lett.* **60**, 1744 (1992).

<sup>15</sup>R. Shneider and R. Auer, *Appl. Phys. Lett.* **67**, 2075 (1995).

<sup>16</sup>K. Tanabe, S. Kubo, F. H. Teherani, H. Asano, and M. Suzuki, *Phys. Rev. Lett.* **72**, 1537 (1994).

<sup>17</sup>W. Kula and R. Sobolewski, *Phys. Rev. B* **49**, 6428 (1994).